Memory responses in visual cortex track recall success after single-trial encoding

Robert Woodry[1], Jonathan Winawer[1,2], Serra Favila[3]

1 Department of Psychology, New York University, New York City, NY 10003

2 Center for Neural Science, New York University, New York City, NY 10003

3 Department of Cognitive and Psychological Sciences, Brown University, Providence, RI 02912

Abstract

Classic models of episodic memory propose that retrieval relies on the reactivation of previous perceptual representations in sensory cortex, a phenomenon known as cortical reinstatement. Supporting this idea, visual memory retrieval has been shown to evoke activity patterns in visual areas similar to those during encoding. However, recent work suggests that memory responses systematically diverge from perceptual ones, challenging this idea. Critically, these studies have focused on highly trained memories, leaving open whether similar effects arise in more naturalistic, single-shot memory scenarios, which are hallmarks of episodic memory. Here, we used fMRI and population receptive field (pRF) modeling to test whether spatially tuned memory responses emerge in early visual cortex after a single encoding event. We scanned 19 participants with fMRI while testing them on their recognition and spatial recall of peripheral objects seen only once. We observed spatially tuned responses in early visual cortex during both recognition and recall, even though spatial location was never explicitly probed during recognition. These responses were better tuned for successfully remembered items, indicating a relationship between neural tuning and behavioral memory performance. Moreover, spatial tuning at encoding predicted subsequent memory: responses for subsequently remembered objects were stronger near the object location and suppressed elsewhere, relative to forgotten items. Taken together, our findings show that a single experience is sufficient to enable spatially tuned reactivation in early visual cortex when remembering an item. Further, our results indicate an important role, during both encoding and retrieval, for early visual cortex representations in successful episodic memory.

Introduction

Episodic memory allows humans to bring to mind the details of a previous experience. In contrast with other learning and memory systems, episodic memory can encode events that have occurred only once and retrieve them with high fidelity. How does the brain achieve this? Dominant models suggest that, at retrieval, pattern completion in the hippocampus leads to the reactivation of neural populations in sensory cortex that were active during the initial encoding of the experience, albeit at a weaker level (Johnson et al., 2009; Polyn et al., 2005; Wheeler et al., 2000). This phenomenon is referred to as cortical reinstatement or reactivation. Indeed, patterns of visually-evoked activity can be used to decode the contents of visual memory in visual areas as early as area V1, suggesting shared patterns of activity during encoding and retrieval (Bosch et al., 2014; Naselaris et al., 2015; Vo et al., 2022). Recent work has shown that lurking beneath the similar patterns of activity during encoding and retrieval, there are also some striking systematic differences. For instance, studies using population receptive field (pRF) modeling techniques have shown that the spatial memory responses in visual cortex are more broadly tuned than their perceptually evoked counterparts, particularly in V1 (Favila et al., 2022; Woodry et al., 2025). Changes in tuning for other visual features, such as spatial frequency, have also been reported (Breedlove et al., 2020). These findings are incompatible with the standard model of cortical reinstatement, as the differences in tuning could be separated from the differences in response amplitude. Instead, these studies indicate that compression of sensory information during the encoding process places constraints on the precision of memory representations and their correspondence to perceptual representations, particularly in the earliest visual areas.

These differences between perceptual and memory representations, while robust, have been studied in a limited range of task contexts, raising questions about their generalizability. In particular, these effects have been reported exclusively in studies that relied on highly-trained associations. Highly-trained associations offer many advantages, such as high task performance and signal-to-noise ratio. However, they do not engage the episodic memory system's most important property: the ability to store a unique, once-experienced event. In addition, highly-trained memories may look different from single-shot memories in visual cortex. In particular, it's possible that spatially tuned responses during recall aren't present immediately, but instead emerge only after repeated precise retrieval practice. This may be especially true in V1, where recall and imagery effects have been more inconsistent than in higher visual areas (Bridge et al., 2012). Another possibility is that repeated retrieval 'fast-tracks' memory consolidation processes that transform memory representations, leading to changes in the memory response that accumulate with retrieval practice (Antony et al., 2017). Thus, a thorough investigation of the differences between perceptual and memory representations in human visual cortex for once-studied memories is needed.

To address these concerns, we sought to extend prior work on representational differences between perception and memory to a single shot memory paradigm, where we could ask: Can spatially tuned memory responses be observed in early visual cortex for items seen just once? We also addressed several secondary questions of interest. First, we assessed whether spatial tuning is related to retrieval demands by comparing two tasks: recognition, where location information is not explicitly probed, and spatial recall, where it is. Second, because single-shot memory paradigms introduce variability in memory behavior, we asked whether spatial tuning is associated with memory performance. Finally, we explored whether our techniques could recover differences in spatial tuning during encoding that predicted subsequent memory. To answer these questions, we scanned human subjects across three tasks. First, they were shown trial-unique objects in the periphery (study). Second, they were asked to identify new vs. old objects (recognition). Last, they were asked to indicate old objects' original locations (recall). We used pRF models to map responses in early visual cortex to visual space across the three different tasks. We find that a single encoding event is sufficient to produce spatially tuned memory responses in early visual cortex, even when spatial location is not explicitly probed. Moreover, these spatially tuned responses map on to memory behavior, where we find better tuned responses for objects whose locations are successfully remembered during recall. We also find effects of spatial tuning at encoding on subsequent memory, where responses for subsequently remembered objects are greater near the object's location and reduced at farther away locations relative to subsequently forgotten items. Collectively, these findings reveal that early visual cortex representations support successful episodic memory during both single-shot encoding and retrieval.

Materials and Methods

Subjects

20 human subjects (12 females, 25-47 years old) were recruited to participate in the experiment and were compensated for their time. One participant was excluded from the analysis because they misunderstood the instructions for providing behavioral responses during the memory task. An initial group of 5 subjects were used for pilot analyses while the remaining 14 were used to validate those analyses. We report here the analyses across all 19 subjects. Subjects were recruited from the New York University community and included the authors S.F. and J.W. Subjects other than the authors were naive to the study's purpose. All subjects gave written informed consent to procedures approved by the New York University Institutional Review Board prior to participation. All subjects had no MRI contraindications, normal color vision, and normal or corrected-to-normal visual acuity.

Stimuli

Object stimuli

This experiment involved testing memory retrieval after a single encoding experience. Therefore, this required the use of a large number of easily recognizable cues with a low probability of confusion. Based on subjective ratings from six subjects not included in the pilot or main experiment, we identified 480 everyday object images from a publicly available dataset that were recognizable in the near periphery (BOSS dataset, (Brodeur et al., 2010). For each set of the three tasks (study, recognition, location), 48 small images of unique objects were sampled without replacement from the 480 images. This produced ten non-overlapping subsets of images — one for each set of three tasks. Within each subset, half (24) were randomly selected without replacement to be used in both the study and location tasks, while the total (48) were used in the recognition task.

On each trial, a small image of one of these objects was shown in either the near periphery (for study trials) or at fixation (for recognition and location trials). During the study task, objects were presented at one of four equispaced peripheral locations around the visual field (45°, 135°, 225°, and 315°) at 2° eccentricity from a central fixation point, spanning 2.5° of visual angle. For the recognition and location tasks, objects were presented at fixation, spanning 1.5° visual angle.

A circular guide spanned the visual field, centered at fixation. This guide consisted of three concentric white circles increasing in radii (2°, 4°, and 6° eccentricity), a horizontal and vertical line that each bisected the circles, and a small white dot at fixation. Object stimuli were presented on top of this guide to provide an external spatial frame of reference.

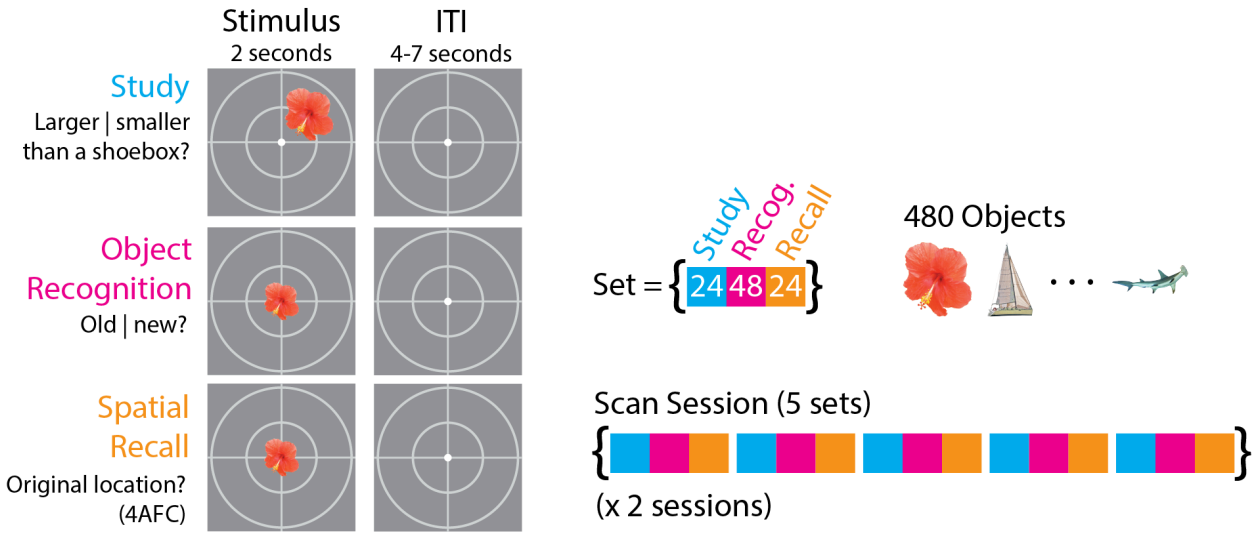

Figure 1. Experimental design

Subjects participated in two fMRI sessions with 15 scans each: study, object recognition, and spatial recall scans, repeated five times (right). The study and recall scans each included 24 trials corresponding to 24 objects, in random order. Recognition scans contained the same 24 objects, with an additional 24 new objects, each shown at fixation in random order. In study trials, subjects were briefly shown objects in one of four locations in the near periphery and asked to indicate whether they were larger or smaller than a shoebox in real life. In recognition trials, subjects were shown both old (studied) and new objects at fixation, and asked to indicate whether they were old or new. In recall trials, subjects were only shown old objects at fixation, and were asked to indicate in which of the four possible locations was the object originally presented.

Experimental Procedure

The experiment cycled through sets of three scans: study, recognition, location. These sets were repeated five times per scan session (Figure 1). Each subject participated in two scan sessions, for a total of 30 scans (10 per task). Study and location scans consisted of 24 trials, one for each object, in random order. Recognition scans consisted of 48 trials, one for each object from the prior study task (old), and another 24 objects not seen before in the experiment (new) — all in random order. Objects in the study task were randomly assigned to, and presented in one of, four peripheral locations. This resulted in a total of 240 trials each for study and location tasks, and 480 trials for recognition tasks, across both scan sessions. Behavioral responses on each trial were collected using a four-response button box. Subjects were instructed to maintain central fixation for all tasks. An EyeLink 1000 Plus eye tracker was used to collect gaze position data and ensure fixation. The eye tracker was mounted onto a rig in the magnet bore that holds the projection screen.

For each study trial, an object was presented in the periphery for 2 seconds. This was followed by an inter-trial interval lasting 4 to 7 seconds. Subjects were instructed to indicate

whether the peripherally presented object was smaller than a shoebox (1), larger than a shoebox (2), or unrecognizable (3).

For each recognition trial, an old (from the prior study task) or new object was presented at fixation for 2 seconds. This was followed by an inter-trial interval lasting 4-7 seconds. Subjects were asked to indicate whether the centrally presented object was old (1), or new (2).

For each location trial, an old object (from the prior study task) was presented at fixation for 2 seconds. This was followed by an inter-trial interval lasting 4-7 seconds. Subjects were asked to indicate the object's original location from the prior study task (1: upper right, 2: lower right, 3: lower left, 4: upper left).

Retinotopic mapping procedure

Each participant additionally underwent 10-12 retinotopic mapping scans in a separate scan session. The stimuli and procedures for the retinotopic mapping session followed those used in Himmelberg et al. (2021), summarized briefly here. Each scan involved contrast patterns presented within bar apertures (1.5° width), which swept across the visual field within a 12°-radius circle. There were 8 bar sweep types in total, comprising 4 diagonal directions and 4 cardinal directions. Each bar sweep took 24s to complete: cardinal sweeps took 24 s to traverse the full extent of the circular aperture; diagonal sweeps took 12 seconds to move to the halfway point, subsequently followed by 12 second long blank periods. Each functional scan comprised 8 sweeps, for a total of 192 seconds. The contrast patterns featured pink noise (grayscale) backgrounds with randomly sized and placed items, updated at 3 Hz. Participants were instructed to press a button whenever the fixation dot changed color, which occurred approximately once every three seconds. These contrast patterns were originally implemented by Benson et al. (2018).

MRI Acquisition

A 3T Siemens Prisma MRI system and a Siemens 64-channel head/neck coil was used to collect functional and anatomical images at the Center for Brain Imaging at New York University. We obtained functional images using a T2*-weighted multiband echo planar imaging (EPI) sequence with whole-brain coverage (repetition time = 1 s, echo time = 37 ms, flip angle = 68°, 66 slices, 2 x 2 x 2 mm voxels, multiband acceleration factor = 6, phase-encoding = posterior-anterior). To estimate and correct susceptibility-induced distortions in the functional EPIs, we collected spin echo images with both anterior-posterior and posterior-anterior phase-encoding. Additionally, for each of the 20 subjects, we acquired one to three whole-brain T1-weighted MPRAGE 3D anatomical volumes (.8 x .8 x .8 mm voxels).

MRI Processing

We used *pydeface* (https://github.com/poldracklab/pydeface) to deface and anonymize all original MRI data (DICOM files). We then used the Heuristic Dicom Converter (Halchenko et

al., 2018) to convert this data to NIFTI and organized the files into the Brain Imaging Data Structure format (K. J. Gorgolewski et al., 2016). We then preprocessed the data using fMRIPrep 20.2.7 (Esteban et al., 2018, 2019), which is based on Nipype 1.7.0 (K. Gorgolewski et al., 2011; K. J. Gorgolewski et al., 2018).

Anatomical data preprocessing.

The following sections on anatomical and functional data preprocessing are provided by the fMRIPrep boilerplate text generated by the preprocessed scan output.

Each of the one to three T1w images was corrected for intensity non-uniformity with N4BiasFieldCorrection (Tustison et al., 2010), distributed with ANTs 2.3.3 (Avants et al., 2008). The T1w-reference was then skull-stripped with a Nipype implementation of the antsBrainExtraction.sh workflow (from ANTs), using OASIS30ANTs as target template. Brain tissue segmentation of cerebrospinal fluid, white-matter and gray-matter was performed on the brain-extracted T1w using fast (FSL 5.0.9, (Zhang et al., 2001)). A T1w-reference map was computed after registration of the T1w images (after intensity non-uniformity-correction) using mri_robust_template (FreeSurfer 6.0.1, (Reuter et al., 2010)). Brain surfaces were reconstructed using recon-all (FreeSurfer 6.0.1, (Dale et al., 1999)), and the brain mask estimated previously was refined with a custom variation of the method to reconcile ANTs-derived and FreeSurfer-derived segmentations of the cortical gray-matter of Mindboggle (Klein, 2017).

Functional data preprocessing.

For each of the 30 BOLD runs found per subject (across all tasks and sessions), the following preprocessing was performed. First, a reference volume and its skull-stripped version were generated by aligning and averaging a single-band reference. A B0-nonuniformity map (or fieldmap) was estimated based on two EPI references with opposing phase-encoding directions, with 3dQwarp (Cox & Hyde, 1997). Based on the estimated susceptibility distortion, a corrected EPI reference was calculated for a more accurate co-registration with the anatomical reference. The BOLD reference was then co-registered to the T1w reference using bbregister (FreeSurfer) which implements boundary-based registration (Greve & Fischl, 2009). Co-registration was configured with six degrees of freedom. Head-motion parameters with respect to the BOLD reference (transformation matrices, and six corresponding rotation and translation parameters) are estimated before any spatiotemporal filtering using mcflirt (FSL 5.0.9, (Jenkinson et al., 2002)). BOLD runs were slice-time corrected to 0.445s (0.5 of slice acquisition range 0s-0.89s) using 3dTshift from AFNI 20160207 (Cox & Hyde, 1997). First, a reference volume and its skull-stripped version were generated using a custom methodology of fMRIPrep. The BOLD time-series were resampled onto the fsnative surface. The BOLD time-series (including slice-timing correction) were resampled onto their original, native space by applying a single, composite transform to correct for head-motion and susceptibility distortions. These resampled BOLD time-series will be referred to as preprocessed BOLD. All resamplings can be performed with a single interpolation step by composing all the pertinent

transformations (i.e. head-motion transform matrices, susceptibility distortion correction, and co-registrations to anatomical and output spaces). Gridded (volumetric) resamplings were performed using antsApplyTransforms (ANTs), configured with Lanczos interpolation to minimize the smoothing effects of other kernels (Lanczos, 1964). Non-gridded (surface) resamplings were performed using mri_vol2surf (FreeSurfer).

Many internal operations of fMRIPrep use Nilearn 0.6.2 (Abraham et al., 2014), mostly within the functional processing workflow. For more details of the pipeline, see the section corresponding to workflows in fMRIPrep's documentation.

General linear models

From each subject's surface based time series, we used GLMSingle (Prince et al., 2022) to estimate the neural pattern of activity during the 2 second stimulus presentations for each trial. GLMsingle first fits to each vertex's time series an optimal response function from a bank of 20 candidate hemodynamic response functions (Natural Scenes Dataset, (Allen et al., 2021)). Second, noisy vertices from the are identified from the data(defined by negative R^2) and then used to estimate noise regressors. This step iteratively uses principal component analysis to derive the noise regressors, an optimal number of noise regressors is chosen and then projected out of the time series' data. Third, fractional ridge regression is used to improve the robustness of single-trial beta estimates, particularly useful here as our design relies on single-trial encoding, recognition, and retrieval of object stimuli.

We constructed three separate design matrices to model the BOLD time series using GLMSingle, one for each of the three tasks. Each of the three design matrices has a regressor corresponding to the object's true location ('target-aligned'). Recognition design matrices had an additional regressor for 'new' objects.

Population receptive field models

Data from the retinotopy session were used to fit a population receptive (pRF) model to each vertex on the cortical surface, as described by Himmelberg et al. ((Himmelberg et al., 2021); section 2.6). To briefly summarize, we fit a circular 2D-Gaussian linear pRF to each surface vertex's BOLD time series, averaged across identical runs of the bar stimulus. These fits were implemented with *Vistasoft* software (Dumoulin & Wandell, 2008), in conjunction with a wrapper function to handle surface data (https://github.com/WinawerLab/prfVista). Gaussian center (x, y) and standard deviation (σ) comprised the pRF model parameters.

Visual field map definitions

We used the visual tool *cortex-annotate* (https://github.com/noahbenson/cortex-annotate), which is built on *neuropythy* software (Benson & Winawer, 2018), to draw and define visual field maps for each subject. To do so, we traced the polar angle reversals on each subject's cortical surface. We followed common heuristics to define four maps spanning early visual cortex: V1, V2, V3 (Benson et al., 2022; Himmelberg et al., 2021). We then defined experiment-specific

regions of interest for each visual field map. To do this we excluded vertices whose variance explained was less than 10% and whose pRF centers were outside one σ of 2° (the target eccentricity in the experiments). For example, a vertex with a pRF center at 1° and pRF size (σ) of 0.5° would be excluded, but a vertex with pRF center at 3° and pRF size of 1.5° deg would be included. We restricted vertices in our analyses this way to examine polar angle activation profiles, described in the next section. These mapping estimates are solely based on the retinotopy scans, and are therefore independent of the main experiment.

Quantifying behavioral performance at recognition and recall

Object recognition

During the recognition task, subjects responded with either 'new' or 'old' for objects presented at fixation. Half of these objects were present in the previous study task ('old'), the rest 'new'. Hits were classified as trials where previously seen objects were correctly identified as 'old'. Misses were classified as trials where previously seen objects were incorrectly identified as 'new'. Correct rejections were classified as trials where new objects were correctly identified as 'new'. False alarms were classified as trials where new objects were incorrectly identified as 'old'. For each scan, the total number of hits were divided by the total number of 'old' objects, to get hit rate as a percentage. Likewise, the total number of false alarms was divided by the total number of 'new' objects to get the false alarm rate as a percentage. Miss and correct rejection rates were calculated as the complement of the hit and false alarm rates, respectively.

Spatial location recall

During the location task, subjects reported which of four locations the object presented at fixation originally appeared at (from the study task). Trials were classified as accurate or inaccurate if the reported location matched that of the original location, or source location, of the object, respectively. Therefore, because all objects shown were 'old' objects that had appeared within the study task in one of four locations, the chance level was at 25%. For each scan, the total number of accurate responses were divided by the number of trials to get mean accuracy.

Analyses quantifying spatial tuning in visual cortex at encoding and retrieval

We computed polar-angle activation profiles for each task (study, recognition, location) across a region of interest comprising visual maps V1, V2, and V3. To do so, we first obtained response amplitudes from the outputs of GLMsingle for each vertex on the cortical surface and each trial. PRF mapping, which was conducted in a separate fMRI session, returned visual field coordinates for each vertex. We excluded vertices not included in the ROI definitions outlined above. We further restricted trials by several criteria: for all tasks, we only included trials where behavioral responses were provided. In the recognition task, we only included trials that were classified as 'hits' (subject reported 'old' when viewing an 'old' object). Some analyses further restricted trials across all tasks to those whose object locations were accurately reported in the recall task. We binned the response amplitudes for the remaining trials and vertices by the

angular distance between each vertex's preferred polar angle and the source location for that object. This binning by angular distance allows for averaging trials across the four peripheral source locations. This produces an activation profile as a function of distance from the object's source location; an activation profile for each subject and task. Each activation profile is then normalized by dividing by the vector length of the perceptually evoked activation profile (from the study task) for the corresponding subject.

Because each subject contributed a different number of trials to each activation profile, we performed two steps to meaningfully aggregate the activation profiles across subjects. First we averaged the normalized activation functions across subjects, weighted by the fraction of trials that each subject contributed towards the group average. We then preserved meaningful units by rescaling each activation profile by the average vector lengths from the study task. Each of the resulting averaged activation profiles peaked near 0°, where values decreased moving away from the peak response. We therefore fit a Von Mises distribution to the averaged activations as a function of angular distance to the source location, θ_{source} (Eq. 1).

$$f(\theta_{source}|\mu, k, s) = s\frac{e^{kcos(\theta_{source}-\mu)}}{2\pi I_0(k)} \qquad \text{Eq. 1}$$

From each of these fits we estimated the peak location, the amplitude (peak to trough), and the width (full-width-at-half-maximum; FWHM). We repeated these analyses, bootstrapping across subjects with replacement 10,000 times to obtain 68% and 95% confidence intervals for each of these three spatial tuning parameter estimates.

Resampling statistics

We analyzed bootstrapped data to infer spatial tuning properties as a function of condition and of other trial-level factors. Statistics reported in this paper are derived from these bootstrapped analyses. We report the mean and confidence intervals (CI) obtained from these analyses to assess our main claims. We report the 95% CI (corresponding to ±2 standard deviations of a normal distribution) when drawing comparisons between a measurement and a fixed value. When comparing two estimates, we instead report the 68% CIs (corr. ±1 standard deviation).

Software

Model fitting, data visualization, and statistical quantification for all analyses described in this paper were made using matplotlib 3.5.2 (Hunter, 2007), nibabel 3.2.2 (Brett et al., 2022), pandas 1.4.2 (The pandas development team, 2024), scikit-learn 1.0.2 (Pedregosa et al., 2011), scipy 1.8.0 (Virtanen et al., 2020), and seaborn 0.11.2 (Waskom, 2021).

Results

We tested whether a single visual event is sufficient for producing spatially tuned memory responses in visual cortex during two kinds of episodic memory retrieval: object recognition and spatial location recall. We also tested whether spatial tuning in visual cortex differs between events where item locations were later remembered or forgotten.

Subjects performed above chance at object recognition and spatial location recall

We first asked whether subjects performed above chance on both the object recognition and the spatial location recall task. In the object recognition task, we computed the hit rate (percentage of 'old' objects identified as 'old') and the false alarm rate (percentage of 'new' objects misidentified as 'old') for each subject. An equal number of objects presented during the object recognition task meant chance performance was at 50%. Subjects achieved an average hit rate of 90% (mean = 0.899, 95 CI [0.87, 0.92]), and an average false alarm rate of 7% (mean = 0.07, 95 CI [0.05, 0.09]), indicating performance well beyond chance level (Figure 2A). Hit and false alarm rates remained stable across scans (Figure 2C).

In the spatial location recall task, we computed the average accuracy for each subject. Because the task had only four options — corresponding to the four potential locations objects could be presented at during the study task — chance performance was at 25%. Subjects achieved an average accuracy of 69% (mean = 0.685, 95 CI [0.63, 0.74], Figure 2B). Subject performance improved the most from the first to the second block, but then leveled off across the rest (Figure 2D).

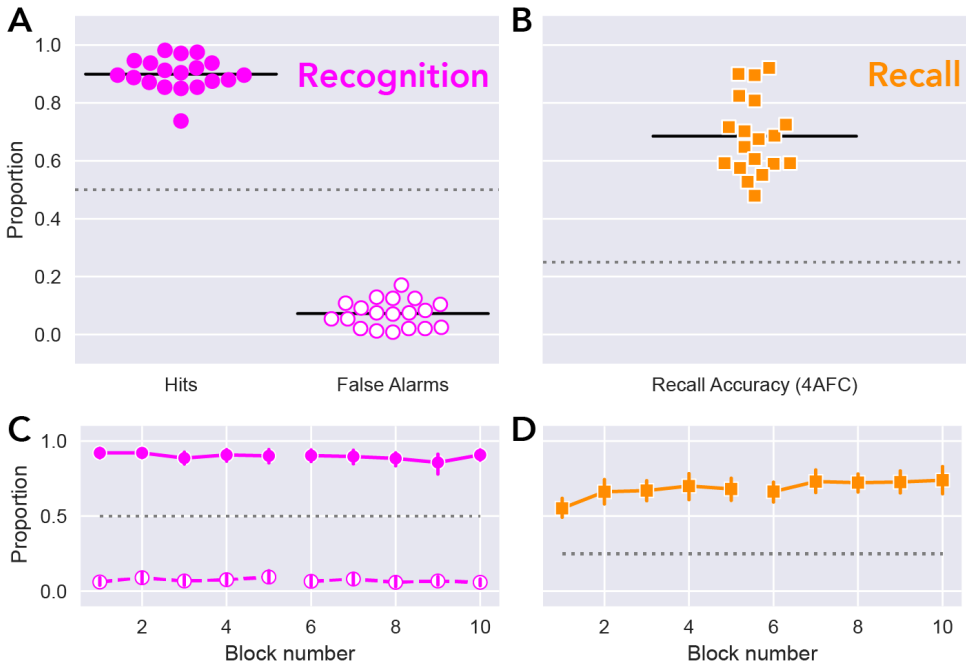

Figure 2. Behavioral performance on object recognition and spatial location recall tasks.
A) Subject-level performance on the object recognition task. Across all subjects (individual points), hit rate (solid pink) and false alarm rate (hollow pink) were well beyond chance (dotted gray line). Black horizontal bars indicate mean hit rate (left) and false alarm rate (right). B) Subject-level performance on the spatial recall task. Across all subjects (individual orange squares), mean performance was well above chance (dotted gray). Black horizontal bar indicates subject group mean. C) Group-level average performance on the object recognition task across blocks. Hit rate (solid pink) and false alarm rate (dashed pink) were stable and well beyond chance (dotted gray) across all blocks and the two sessions. Error bars indicate 95% CI obtained from 1000 bootstraps across subjects. D) Group-level average performance on the spatial recall task across blocks. Mean performance was stable and well beyond chance (dotted gray) across all blocks and the two sessions. Error bars indicate 95% CI obtained from 1000 bootstraps across subjects.

A single viewing is sufficient for spatially tuned memory responses in early visual cortex

Confident that our subjects could recognize objects and retrieve their original location after a single viewing, we next asked whether retrieving these object memories could produce activity in visual cortex spatially tuned to the object's source location. We tested this hypothesis by remapping estimates of brain activity from the surface of early visual cortex (V1-V3) to visual space. From these we computed polar angle activation profiles for each visual map and task, and quantified each profile's spatial tuning by computing its peak location, amplitude, and tuning width.

Across each task, activity in V1-V3 in each task was spatially tuned to the object's peripheral location (study = -1°, 95 CI [-2°, 0.5°]; recognition = -9°, 95 CI [-31°, 9°]; recall =

-13°, 95 CI [-47°, 22°]; Figure 3A). Though a Von Mises function fit to the response during study captured more of the variance in activity compared to fits to responses during recognition (mean R^2 diff = 0.29, 95 CI [0.07, 0.65]) and during recall (mean R^2 diff = 0.4, 95 CI [0.12, 0.81]), the fits still captured most of the variance in each task (study R^2: 0.99, recognition R^2: 0.78, recall R^2: 0.73, Figure 3B). The fact that each memory response produced activity that clearly peaks near the studied location (0°) confirms our hypothesis that a single encoding event is sufficient to produce spatially tuned responses in early visual cortex during memory retrieval. Interestingly, this was observed during both recall and recognition tasks, even though location was not explicitly relevant for the recognition judgment.

We next asked how the spatial tuning parameters of the memory retrieval responses compared to those from encoding. First, we compared the estimates of peak location: we found that, compared to the encoding response, the absolute error (distance of the peak location to 0°) of the memory response was larger during both recognition (mean diff = 10°, 95 CI [-1°, 30°]) and recall (mean diff = 16°, 95 CI [-1°, 47°]; Figure 3C). Second, the response at encoding also had a substantially larger amplitude than the responses during recognition (mean diff = 0.86, 95 CI [0.71, 1.03]) and during recall (mean diff = 0.87, 95 CI [0.72, 1.03]; Figure 3D). Lastly, the responses during both memory retrieval tasks were more broadly tuned compared to the response at encoding (study = 81°, 68 CI [79°, 83°], recognition = 122°, 68 CI [94°, 138°]; recall = 162°, 68 CI [107°, 178°]; Figure 3E), consistent with our prior work (Favila et al., 2022; Woodry et al., 2025).

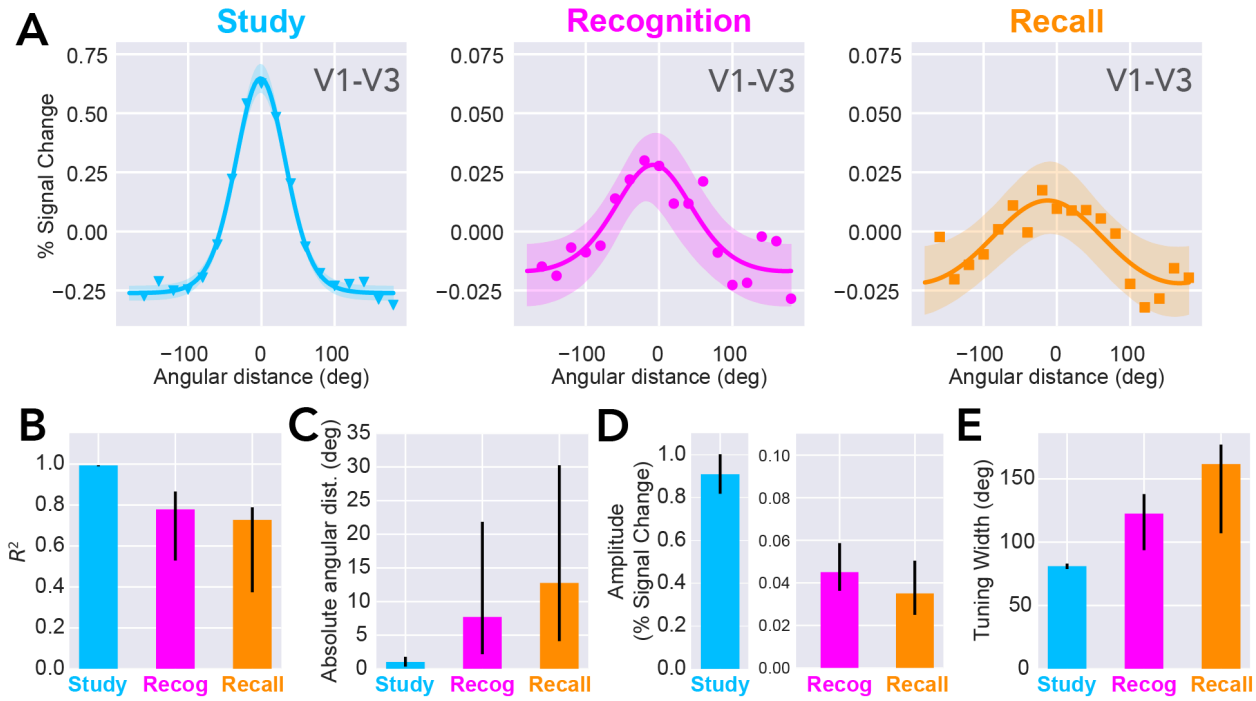

Figure 3. Single-shot memory responses in visual cortex are tuned to encoded location.
A) Polar angle activation profiles fit to brain activity in early visual cortex. Shaded region indicates 68% confidence interval across subjects. While the spatial tuning of responses at encoding are predictably good, the responses during both retrieval tasks were remarkably tuned to the studied object location, even though the object was only shown at that location once. B-E) Estimates of tuning quality observed during single-trial encoding, recognition, and recall. Error bars indicate 68% bootstrapped confidence intervals across subjects. B) Variance explained for each task's Von Mises fit. While noisier than at encoding, the fits to memory responses at retrieval accounted for at least 70% of the variance. C) Absolute distance between peak location and object source location. Responses at retrieval were less accurate than responses at encoding, but were still reasonably aligned to the object's source location. D) The amplitude (peak to trough) of responses at retrieval were less than a tenth of those at encoding, yet comfortably above zero. E) The tuning width of responses at memory retrieval were characteristically broader than at encoding, consistent with previous studies.

Memory responses in early visual cortex track locations of remembered objects

To test if the presence of spatially tuned memory responses in visual cortex predicts successful recall, we grouped trials in each memory task by whether the object's location was later remembered or forgotten (behavioral report during recall, Figure 4A), recomputing the polar angle activation profile for each (Figure 4B). These profiles reveal clear spatial tuning for the memory response, both during recognition and recall, when the object's location is successfully remembered. In contrast, the memory response is less tuned for trials where the object's location is forgotten, particularly during the recall task. Indeed, when object location is forgotten, the estimates of peak location are further away from the target when compared to trials where the object location was successfully remembered (recognition mean diff = 43°, 95

CI [-7°, 107°]; recall mean diff = 90°, 95 CI [21°, 173°]; Figure 4C Right). We also find that the variance explained in model fits tends to be somewhat but not reliably lower during both recognition (mean diff = -0.21, 95 CI [-0.69, 0.32]) and recall (mean diff = -0.29, 95 CI [-0.77, 0.27]; Figure 4C Left). These results show that accurate spatial tuning of memory responses in early visual cortex is associated with accurate spatial recall.

While the exclusion of forgotten trials does not impact the tuning of the recognition response, it does marginally improve some aspects of the spatial tuning of the recall response (R^2 diff = 0.12, 95 CI [-0.02, 0.31]; absolute error diff = -8°, 95 CI [-32°, 5°]; amplitude diff = 0.02, 95 CI [0.01, 0.03]; width diff = -29°, 95 CI [-87, 27°]). One may be inclined to propose, then, that the observation of broader tuning during memory vs. encoding for all trials (Figure 3E) could instead be due to the inclusion of inaccurately retrieved memory responses. However, when we compare the memory responses for only remembered objects to the response at encoding, we find that this is not the case: response tuning remains broader during both retrieval tasks than during the study task (study = 81°, 68 CI [79°, 83°], recognition = 122°, 68 CI [100°, 140°]; recall = 133°, 68 CI [97°, 151°]).

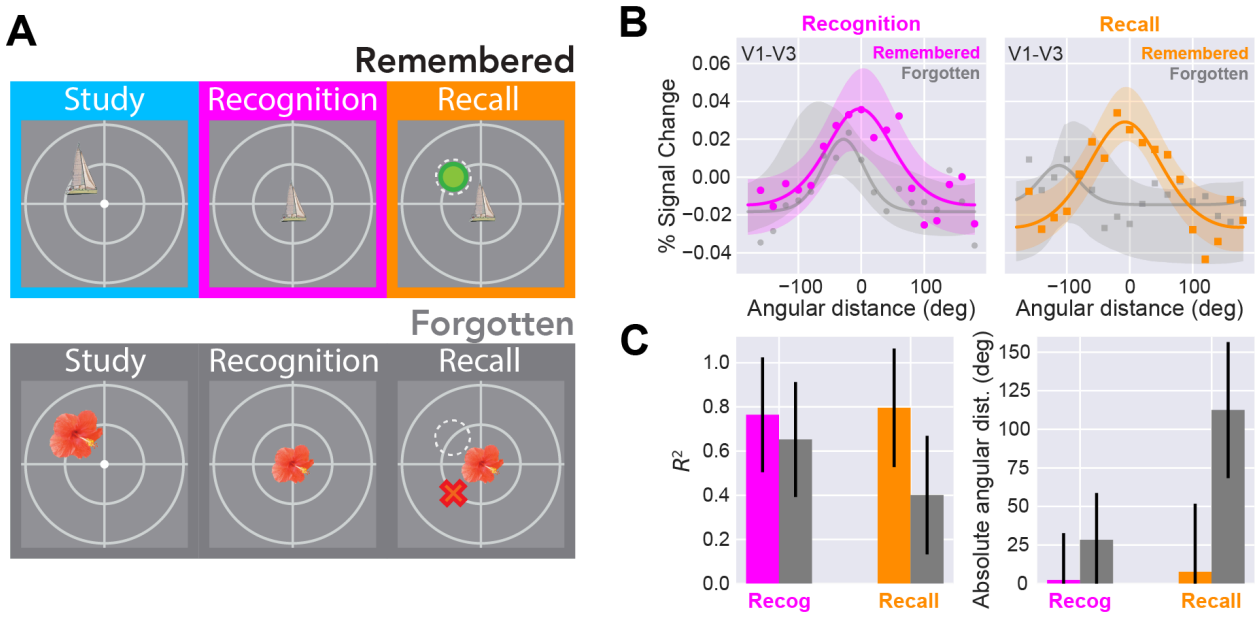

Figure 4. Spatially-tuned memory responses in early visual cortex track recall success

A) Schematic for grouping subsequently remembered/forgotten trials across tasks. Trials in each task (study, recognition, and recall) are assigned to the 'remembered' group if the object's location is subsequently reported correctly during the recall task. Trials are deemed 'forgotten' if location is reported incorrectly during the recall task. B) Polar angle activation profiles fit to brain activity in early visual cortex, split by whether the object's location was later remembered (pink, orange) vs. forgotten (gray) at recall. Clearer tuning to the object's source location for subsequently remembered object locations, especially for the recall task. C) Variance explained (left) and absolute peak location error (right) for fits to memory responses split by whether the object's location was later remembered vs. forgotten. Error bars denote standard deviation of the bootstrapped difference in R^2 (left) and angular error in peak location (right) between remembered and forgotten groups. While variance explained appears to drop slightly, absolute error in peak location is larger for the forgotten than for the remembered trials.

Spatial tuning at encoding predicts subsequent memory

Objects whose locations were later forgotten during the recall task may differ in how they were encoded, reflected by differences in cortical activity during stimulus encoding. Previous research has generally failed to observe this subsequent memory effect in early visual cortex (Kim, 2011). However, because early visual cortex is highly spatially selective, standard univariate tests which pool evoked activity across early visual areas likely average spatially localized differences in the response at encoding. Here our encoding model-based analyses provide an advantage. Our analyses respect the spatial selectivity in visual cortex by mapping cortical responses to visual space and aligning these responses to the spatial location of stimulus, preserving the spatial selectivity across encoding trials. We therefore hypothesized that we could reveal any subsequent memory effects in early visual cortex by grouping study trials according to whether the object's location was later forgotten or remembered.

We tested this hypothesis by comparing the activation profiles between the remembered and forgotten groups during the study task (Figure 5A). From these initial comparisons we find larger responses at encoding in each visual area for trials whose object locations were later remembered than for those later forgotten. Indeed, we find consistently larger amplitude estimates across early visual cortex for remembered vs. forgotten trials (mean diff = 0.11% signal change, 95 CI [0.01, 0.21]). Additionally, we find that this subsequent memory effect is spatially selective: by taking the difference of binned activations between remembered and forgotten trials, we observe 1) a gain in the response localized near the target, and 2) a reduction of the surround response (Figure 5C). This effect on the population tuning response in early visual cortex is consistent with work on attention (Tünçok et al., 2024), raising the possibility that attentional signals could be modulating the response at encoding, thereby improving memory of the stimulus.

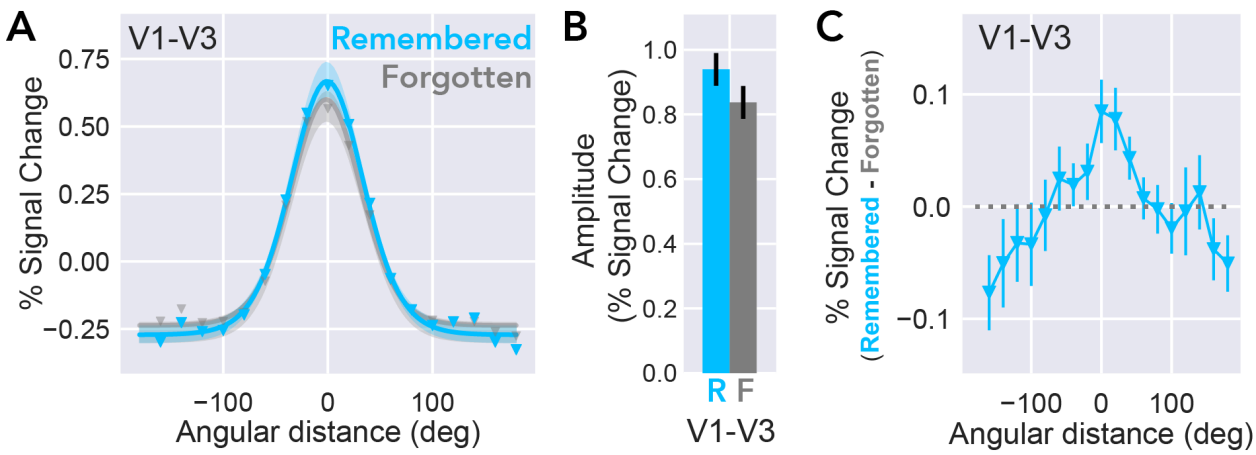

Figure 5. Spatial tuning in early visual cortex at encoding predicts subsequent recall

A) Polar angle activation profiles fit to brain activity across early visual cortex at encoding (study), grouped by whether the encoded object's location was later remembered (blue) or forgotten (gray) at recall. Shaded region indicates 68% confidence interval across subjects. B) Amplitude estimates (peak to trough) at encoding for remembered and forgotten groups. Error bars indicate one standard deviation of the amplitude difference between the two groups across bootstraps. C) Differences in BOLD response between remembered and forgotten groups as a function of angular distance to the target. Error bars indicate one standard deviation of the bootstrapped differences between the two groups.

Discussion

We measured the spatial tuning of visual cortical responses during object encoding, recognition, and recall — with only a single encoding event for each stimulus. We demonstrated that a single encoding experience is sufficient to produce spatially tuned memory responses in visual cortex during later memory retrieval. We further showed that these spatially tuned responses do not require spatial information being explicitly probed, indicating that such responses can arise spontaneously. Lastly, we found that successful spatial recall is associated with both a) the presence of spatially tuned responses in visual cortex during recall, and b) changes to spatial tuning during encoding – specifically, enhanced responses near the object location and reduced responses elsewhere.

Our findings advance previous work using encoding models to study memory reactivation (Favila et al., 2022; Favila & Aly, 2023; Woodry et al., 2025). Here, we demonstrate that a single encoding event is sufficient to generate spatially specific responses in early visual cortex during retrieval. This contrasts with prior studies that have relied on highly practiced stimulus-response associations, often involving many rounds of retrieval practice and/or feedback-based learning (Bosch et al., 2014; Favila et al., 2022; Vo et al., 2022; Woodry et al., 2025). While frequent practice is useful for generating high levels of performance, it does not engage the episodic memory system's core function: storing and retrieving information about unique, once-experienced events. By showing that spatially tuned responses can be observed in early visual cortex after a single viewing, our results suggest that memories are reflected in early sensory regions even in the absence of training or repetition.

Strikingly, spatially tuned responses in visual cortex emerged even during recognition, when spatial location was not relevant to the task. This suggests that reactivation of perceptual representations can sometimes occur even in the absence of explicit retrieval demands for spatial information. Such spontaneous reinstatement could imply that memory retrieval involves the reconstruction of a richer, more complete representation than is strictly required for task performance, or that other regions besides early visual cortex align these representations with task demands (Favila et al., 2018; Kuhl et al., 2013; Kwak & Curtis, 2022). However, it's also important to note that participants in our experiment knew that they would ultimately be tested on object locations, and thus may have been strategically recalling this information in preparation for this later task. Future studies will need to further characterize how reactivation interacts with retrieval demands, for example with a surprise recall task.

Our results further revealed that the presence and quality of spatial tuning in early visual cortex were linked to recall success. During recall, spatially tuned responses were robust for items whose locations were successfully remembered and disorganized for items whose locations were forgotten. This pattern of data is consistent with prior studies that have linked decoded memory content to recall behavior (Gordon et al., 2014; Kuhl et al., 2011; Polyn et al.,

2005). However, decoding methods are limited by their inability to separate out the effects of signal-to-noise-ratio and the precision of the memory response — any combination of which would decrease decoder performance. Instead, our use of encoding models allows us to separately characterize the amplitude, precision (width), and accuracy (peak location) of the memory response as it relates to successful recall. During recognition, we saw more limited tuning differences between successfully recognized objects whose spatial location was later recalled and successfully recognized objects whose spatial location was later forgotten. The presence of some tuning for subsequently forgotten items could reflect forgetting of some locations that were reactivated during recognition prior to the spatial recall test.

Interestingly, we also found that tuning differences related to recall were evident at encoding: subsequently remembered items elicited stronger responses near the object's location and weaker responses elsewhere compared to subsequently forgotten items. These encoding-related differences could reflect the operation of attentional mechanisms that enhance the neural representation of relevant information (Kensinger et al., 2003; Uncapher & Rugg, 2009; Uncapher & Wagner, 2009). While we did not directly manipulate attention in this study, limiting our ability to draw strong conclusions about it here, there are several reasons for our interpretation. First, selective attention is known to modulate activity in early visual cortex in a similar manner to what we observed (Ling et al., 2015; Tootell et al., 1998; Tünçok et al., 2024). Second, attention has been repeatedly implicated in promoting memory encoding (Craik et al., 1996; Uncapher & Wagner, 2009; Wager et al., 2004). Notably, prior work on subsequent memory effects has not typically implicated early visual cortex (Kim, 2011). However, it is important to note that most papers look for univariate differences present across entire regions of interest. Here, we see small, but robust, subsequent memory effects at specific visual field locations which change on each trial, and which would be obscured by averaging over all of early visual cortex.

Collectively, this work makes progress on characterizing memory reactivation in human visual cortex in a single-shot encoding paradigm that echoes the demands of real world episodic memory. We demonstrate a role for early visual cortex in promoting successful encoding and retrieval of episodic memories in this context.

REFERENCES

Abraham, A., Pedregosa, F., Eickenberg, M., Gervais, P., Mueller, A., Kossaifi, J., Gramfort, A., Thirion, B., & Varoquaux, G. (2014). Machine learning for neuroimaging with scikit-learn. *Frontiers in Neuroinformatics*, *8*, 14.

Allen, E. J., St-Yves, G., Wu, Y., Breedlove, J. L., Prince, J. S., Dowdle, L. T., Nau, M., Caron, B., Pestilli, F., Charest, I., Hutchinson, J. B., Naselaris, T., & Kay, K. (2021). A massive 7T fMRI dataset to bridge cognitive neuroscience and artificial intelligence. *Nature Neuroscience*, *25*(1), 116–126.

Antony, J. W., Ferreira, C. S., Norman, K. A., & Wimber, M. (2017). Retrieval as a fast route to memory consolidation. *Trends in Cognitive Sciences*, *21*(8), 573–576.

Avants, B. B., Epstein, C. L., Grossman, M., & Gee, J. C. (2008). Symmetric diffeomorphic image registration with cross-correlation: evaluating automated labeling of elderly and neurodegenerative brain. *Medical Image Analysis*, *12*(1), 26–41.

Benson, N. C., & Winawer, J. (2018). Bayesian analysis of retinotopic maps. *eLife*, *7*. https://doi.org/10.7554/eLife.40224

Benson, N. C., Yoon, J. M. D., Forenzo, D., Engel, S. A., Kay, K. N., & Winawer, J. (2022). Variability of the Surface Area of the V1, V2, and V3 Maps in a Large Sample of Human Observers. *The Journal of Neuroscience: The Official Journal of the Society for Neuroscience*, *42*(46), 8629–8646.

Bosch, S. E., Jehee, J. F. M., Fernández, G., & Doeller, C. F. (2014). Reinstatement of associative memories in early visual cortex is signaled by the hippocampus. *The Journal of Neuroscience: The Official Journal of the Society for Neuroscience*, *34*(22), 7493–7500.

Breedlove, J. L., St-Yves, G., Olman, C. A., & Naselaris, T. (2020). Generative Feedback Explains Distinct Brain Activity Codes for Seen and Mental Images. *Current Biology: CB*, *30*(12), 2211–2224.e6.

Brett, M., Markiewicz, C. J., Hanke, M., Côté, M.-A., Cipollini, B., McCarthy, P., Jarecka, D., Cheng, C. P., Halchenko, Y. O., Cottaar, M., Larson, E., Ghosh, S., Wassermann, D., Gerhard, S., Lee, G. R., Wang, H.-T., Kastman, E., Kaczmarzyk, J., Guidotti, R., … freec84. (2022). nipy/nibabel: 3.2.2 (3.2.2). Zenodo. https://doi.org/10.5281/zenodo.6617121

Bridge, H., Harrold, S., Holmes, E. A., Stokes, M., & Kennard, C. (2012). Vivid visual mental imagery in the absence of the primary visual cortex. *Journal of Neurology*, *259*(6), 1062–1070.

Brodeur, M. B., Dionne-Dostie, E., Montreuil, T., & Lepage, M. (2010). The Bank of Standardized Stimuli (BOSS), a new set of 480 normative photos of objects to be used as visual stimuli in cognitive research. *PloS One*, *5*(5), e10773.

Cox, R. W., & Hyde, J. S. (1997). Software tools for analysis and visualization of fMRI data. *NMR in Biomedicine*, *10*(4-5), 171–178.

Craik, F. I., Govoni, R., Naveh-Benjamin, M., & Anderson, N. D. (1996). The effects of divided attention on encoding and retrieval processes in human memory. *Journal of Experimental Psychology. General*, *125*(2), 159–180.

Dale, A. M., Fischl, B., & Sereno, M. I. (1999). Cortical surface-based analysis. I. Segmentation and surface reconstruction. *NeuroImage*, *9*(2), 179–194.

Dumoulin, S. O., & Wandell, B. A. (2008). Population receptive field estimates in human visual cortex. *NeuroImage*, *39*(2), 647–660.

Esteban, O., Blair, R., Markiewicz, C. J., Berleant, S. L., Moodie, C., Ma, F., Isik, A. I., Erramuzpe, A., Kent, J. D., Goncalves, M., & Others. (2018). fMRIPrep. Software. *Zenodo*.

Esteban, O., Markiewicz, C. J., Blair, R. W., Moodie, C. A., Isik, A. I., Erramuzpe, A., Kent, J. D., Goncalves, M., DuPre, E., Snyder, M., Oya, H., Ghosh, S. S., Wright, J., Durnez, J., Poldrack, R. A., & Gorgolewski, K. J. (2019). fMRIPrep: a robust preprocessing pipeline for functional MRI. *Nature Methods*, *16*(1), 111–116.

Favila, S. E., & Aly, M. (2023). Hippocampal mechanisms resolve competition in memory and perception. *bioRxiv.org: The Preprint Server for Biology*. https://doi.org/10.1101/2023.10.09.561548

Favila, S. E., Kuhl, B. A., & Winawer, J. (2022). Perception and memory have distinct spatial tuning properties in human visual cortex. *Nature Communications*, *13*(1), 5864.

Favila, S. E., Samide, R., Sweigart, S. C., & Kuhl, B. A. (2018). Parietal representations of stimulus features are amplified during memory retrieval and flexibly aligned with top-down goals. *The Journal of Neuroscience: The Official Journal of the Society for Neuroscience*, *38*(36), 7809–7821.

Gordon, A. M., Rissman, J., Kiani, R., & Wagner, A. D. (2014). Cortical reinstatement mediates the relationship between content-specific encoding activity and subsequent recollection decisions. *Cerebral Cortex* , *24*(12), 3350–3364.

Gorgolewski, K., Burns, C. D., Madison, C., Clark, D., Halchenko, Y. O., Waskom, M. L., & Ghosh, S. S. (2011). Nipype: a flexible, lightweight and extensible neuroimaging data processing framework in python. *Frontiers in Neuroinformatics*, *5*, 13.

Gorgolewski, K. J., Auer, T., Calhoun, V. D., Craddock, R. C., Das, S., Duff, E. P., Flandin, G., Ghosh, S. S., Glatard, T., Halchenko, Y. O., Handwerker, D. A., Hanke, M., Keator, D., Li, X., Michael, Z., Maumet, C., Nichols, B. N., Nichols, T. E., Pellman, J., … Poldrack, R. A. (2016). The brain imaging data structure, a format for organizing and describing outputs of neuroimaging experiments. *Scientific Data*, *3*(1), 1–9.

Gorgolewski, K. J., Nichols, T., Kennedy, D. N., Poline, J.-B., & Poldrack, R. A. (2018). Making replication prestigious. *The Behavioral and Brain Sciences*, *41*, e131.

Greve, D. N., & Fischl, B. (2009). Accurate and robust brain image alignment using boundary-based registration. *NeuroImage*, *48*(1), 63–72.

Halchenko, Y. O. et al. (2018). Open Source Software: Heudiconv. *Zenodo*, https://doi.org/10.5281/zenodo.1306159.

Himmelberg, M. M., Kurzawski, J. W., Benson, N. C., Pelli, D. G., Carrasco, M., & Winawer, J. (2021). Cross-dataset reproducibility of human retinotopic maps. *NeuroImage*, *244*, 118609.

Hunter J, (2007). Matplotlib: A 2D Graphics Environment. *Computing in Science & Engineering*, *9*(3), 90-95

Jenkinson, M., Bannister, P., Brady, M., & Smith, S. (2002). Improved optimization for the robust and accurate linear registration and motion correction of brain images. *NeuroImage*, *17*(2), 825–841.

Johnson, J. D., McDuff, S. G. R., Rugg, M. D., & Norman, K. A. (2009). Recollection, familiarity, and cortical reinstatement: a multivoxel pattern analysis. *Neuron*, *63*(5), 697–708.

Kensinger, E. A., Clarke, R. J., & Corkin, S. (2003). What neural correlates underlie successful encoding and retrieval? A functional magnetic resonance imaging study using a divided attention paradigm. *The Journal of Neuroscience: The Official Journal of the Society for Neuroscience*, *23*(6), 2407–2415.

Kim, H. (2011). Neural activity that predicts subsequent memory and forgetting: a meta-analysis of 74 fMRI studies. *NeuroImage*, *54*(3), 2446–2461.

Klein, A. (2017). *Mindboggle-101 templates (unlabeled images from a population of brains). Harvard Dataverse*.

Kuhl, B. A., Johnson, M. K., & Chun, M. M. (2013). Dissociable neural mechanisms for goal-directed versus incidental memory reactivation. *The Journal of Neuroscience: The Official Journal of the Society for Neuroscience*, *33*(41), 16099–16109.

Kuhl, B. A., Rissman, J., Chun, M. M., & Wagner, A. D. (2011). Fidelity of neural reactivation reveals competition between memories. *Proceedings of the National Academy of Sciences of the United States of America*, *108*(14), 5903–5908.

Kwak, Y., & Curtis, C. E. (2022). Unveiling the abstract format of mnemonic representations. *Neuron*, *110*(11), 1822–1828.e5.

Lanczos, C. (1964). Evaluation of Noisy Data. *Journal of the Society for Industrial and Applied Mathematics Series B Numerical Analysis*, *1*(1), 76–85.

Ling, S., Jehee, J. F. M., & Pestilli, F. (2015). A review of the mechanisms by which attentional feedback shapes visual selectivity. *Brain Structure & Function*, *220*(3), 1237–1250.

Naselaris, T., Olman, C. A., Stansbury, D. E., Ugurbil, K., & Gallant, J. L. (2015). A voxel-wise encoding model for early visual areas decodes mental images of remembered scenes. *NeuroImage*, *105*, 215–228.

Pedregosa, F., Varoquaux, G., Gramfort, A., Michel, V., Thirion, B., Grisel, O., Blondel, M., Louppe, G., Prettenhofer, P., Weiss, R., Weiss, R. J., Vanderplas, J., Passos, A., Cournapeau, D., Brucher, M., Perrot, M., & Duchesnay, E. (2011). Scikit-learn: Machine Learning in Python. *Journal of Machine Learning Research: JMLR*, *abs/1201.0490*. https://doi.org/10.5555/1953048.2078195

Polyn, S. M., Natu, V. S., Cohen, J. D., & Norman, K. A. (2005). Category-specific cortical activity precedes retrieval during memory search. *Science (New York, N.Y.)*, *310*(5756), 1963–1966.

The pandas development team. (2024). pandas-dev/pandas: Pandas (v2.2.1). Zenodo. https://doi.org/10.5281/zenodo.10697587

Prince, J. S., Charest, I., Kurzawski, J. W., Pyles, J. A., Tarr, M. J., & Kay, K. N. (2022). Improving the accuracy of single-trial fMRI response estimates using GLMsingle. *eLife*, *11*. https://doi.org/10.7554/eLife.77599

Reuter, M., Rosas, H. D., & Fischl, B. (2010). Highly accurate inverse consistent registration: a robust approach. *NeuroImage*, *53*(4), 1181–1196.

Tootell, R. B., Hadjikhani, N., Hall, E. K., Marrett, S., Vanduffel, W., Vaughan, J. T., & Dale, A. M. (1998). The retinotopy of visual spatial attention. *Neuron*, *21*(6), 1409–1422.

Tünçok, E., Carrasco, M., & Winawer, J. (2024). Spatial attention alters visual cortical representation during target anticipation. In *bioRxiv*. https://doi.org/10.1101/2024.03.02.583127

Tustison, N. J., Avants, B. B., Cook, P. A., Zheng, Y., Egan, A., Yushkevich, P. A., & Gee, J. C. (2010). N4ITK: improved N3 bias correction. *IEEE Transactions on Medical Imaging*, *29*(6), 1310–1320.

Uncapher, M. R., & Rugg, M. D. (2009). Selecting for memory? The influence of selective attention on the mnemonic binding of contextual information. *The Journal of Neuroscience: The Official Journal of the Society for Neuroscience*, *29*(25), 8270–8279.

Uncapher, M. R., & Wagner, A. D. (2009). Posterior parietal cortex and episodic encoding: insights from fMRI subsequent memory effects and dual-attention theory. *Neurobiology of Learning and Memory*, *91*(2), 139–154.

Virtanen, P., Gommers, R., Oliphant, T. E., Haberland, M., Reddy, T., Cournapeau, D., Burovski, E., Peterson, P., Weckesser, W., Bright, J., van der Walt, S. J., Brett, M., Wilson, J., Millman, K. J., Mayorov, N., Nelson, A. R. J., Jones, E., Kern, R., Larson, E., … van Mulbregt, P. (2020). SciPy 1.0: fundamental algorithms for scientific computing in Python. *Nature Methods*, *17*(3), 261–272.

Vo, V. A., Sutterer, D. W., Foster, J. J., Sprague, T. C., Awh, E., & Serences, J. T. (2022). Shared representational formats for information maintained in working memory and information retrieved from long-term memory. *Cerebral Cortex* , *32*(5), 1077–1092.

Wager, T. D., Jonides, J., & Reading, S. (2004). Neuroimaging studies of shifting attention: a meta-analysis. *NeuroImage*, *22*(4), 1679–1693.

Waskom, M. L., (2021). seaborn: statistical data visualization. Journal of Open Source Software, 6(60), 3021, https://doi.org/10.21105/joss.03021

Wheeler, M. E., Petersen, S. E., & Buckner, R. L. (2000). Memory's echo: vivid remembering reactivates sensory-specific cortex. *Proceedings of the National Academy of Sciences of the United States of America*, *97*(20), 11125–11129.

Woodry, R., Curtis, C. E., & Winawer, J. (2025). Feedback scales the spatial tuning of cortical responses during both visual working memory and long-term memory. *The Journal of Neuroscience: The Official Journal of the Society for Neuroscience*. https://doi.org/10.1523/JNEUROSCI.0681-24.2025

Zhang, Y., Brady, J. M., & Smith, S. M. (2001). An hmrf-em algorithm for partial volume segmentation of brain mri fmrib technical report tr01yz1. *Brain: A Journal of Neurology*. https://www.fmrib.ox.ac.uk/datasets/techrep/tr01yz1/tr01yz1.pdf